Desalination and Water Treatment
www.deswater.com

doi: 10.5004/dwt.2019.23361

140 (2019) 163–171
February

Removal of boron from aqueous solutions using electrospun PVDF nanofibrous adsorbent modified by poly(glycidyl methacrylate)/glucamine ligands

Madana Leela Nallappan[a], Mohamad Mahmoud Nasef[b,*], Teo Ming Ting[c,*], Arshad Ahmad[d]

[a]*Faculty of Chemical Engineering, Universiti Teknologi Malaysia, 81310 UTM Johor Bahru, Johor, Malaysia*
[b]*Chemical Engineering Department, Universiti Teknologi PETRONAS, 32610 Seri Iskander, Perak, Malaysia, emails: mohamed.nasef@utp.edu.my, mahmoudeithar@cheme.utm.my*
[c]*Radiation Technology Division, Malaysian Nuclear Agency, 43000 Kajang, Selangor, Malaysia, email: tmting@nm.gov.my*
[d]*Center of Hydrogen Energy, Institute of Future Energy, Universiti Teknologi Malaysia, 81310 UTM Johor Bahru, Johor, Malaysia*

Received 3 May 2018; Accepted 26 October 2018

ABSTRACT

The removal of boron from aqueous solutions using nanofibrous adsorbent containing grafted poly(glycidyl methacrylate) with glucamine ligand was investigated in a batch equilibration mode. Particularly, the equilibrium isotherms, kinetics, thermodynamics of boron adsorption onto a newly prepared chelating adsorbent obtained by radiation-induced grafting of glycidyl methacrylate onto electrospun poly(vinylidene fluoride) nanofibers followed by chemical treatment with *N*-methyl-*D*-glucamine were studied. The equilibrium data were fitted to the Langmuir, Freundlich and Redlich–Peterson isotherms, whereas the kinetic data were tested with the pseudo-first-order and pseudo-second-order kinetic models. The adsorption thermodynamic parameters such as Gibbs free energy change (ΔG), enthalpy changes (ΔH), and entropy changes (ΔS) were also determined. The adsorption data were best represented by Redlich–Peterson isotherm model, and the kinetics were well expressed by the pseudo-second-order model. The boron adsorption on the nanofibrous adsorbent occurred spontaneously on chemisorption basis and is governed by the film diffusion mechanism. The overall findings suggest that the newly prepared nanofibrous adsorbent have a strong potential for boron removal from aqueous solutions.

Keywords: Boron chelating nanofibrous adsorbent; Electrospun PVDF; Adsorption kinetics; Adsorption isotherms; Adsorption mechanism

1. Introduction

The widespread applications of boron in various industries including nuclear technology, rocket fuel making, and production of heat-resistant materials, ceramics, glass, detergents, disinfectants, dyestuff, fertilizers, and food preservatives have left water streams contaminated with excessive amounts of boron causing health and environmental concerns [1]. A value of 2.4 mg/L was set by the World Health Organization for drinking water [2] whereas a value <4.0 mg/L was set by a number of countries across the world for boron in the wastewater discharge [1]. Therefore, increasing efforts to search for efficient, cost-effective boron chelating materials and robust systems for the removal of boron from different water streams have attracted worldwide attention.

Various separation techniques such as adsorption–coagulation [3–5], electrocoagulation [6], electrodialysis [7,8], reverse osmosis [9], and ion chelation [10] have been applied for boron removal. Off all, ion chelation with selective resins containing *N*-methyl-*D*-glucamine (NMDG) have been found highly effective in boron removal and achieving dischargeable low boron levels in the treated streams compared with other technologies [11]. The presence of five hydroxyl groups

* Corresponding authors.

1944-3994/1944-3986 © 2019 Desalination Publications. All rights reserved.

in NMDG permits boron binding through a covalent bond forming a stable coordination complex, and the bound boron can be released by the treatment with a solution of strong acid (e.g., HCl) allowing resin's regeneration. Therefore, majority of the commercial resins for this application contain NMDG as the functional group [10,11]. Nevertheless, such commercial resins are challenged by slow kinetics and relatively low boron uptake capacity despite their high selectivity to boric acid in regions with neutral pH levels [12,13]. Moreover, such resins have relatively high cost and loss of capacity upon scaling up [14,15] in addition to limited surface areas, uncontrollable pore structures, and high hydrophobicity making the process of boron removal less flexible and the performance unsatisfactorily [16,17]. This triggered various research efforts to develop alternative boron chelating adsorbents with improved performance.

Recent studies showed that boron chelating adsorbents with fibrous structure have more efficient boron removal compared with granular resins [18–23]. Particularly, adsorbents obtained by grafting based on polyethylene-coated polypropylene (PE-PP) [18,20,21] nylon-6 [19,22], PP, and viscose [23] microfibers showed higher boron adsorption capacity and faster kinetics than conventional resins. Among grafting methods, radiation-induced grafting (RIG) is a convenient technique to produce precursors that could be converted to boron-selective adsorbents after functionalization with desired level of ionic groups in large quantities [20,21]. For example, monomers such as glycidyl methacrylate (GMA) [18] and vinylbenzyl chloride (VBC) [22] were grafted onto PE-PP microfibers (average diameter of 30–50 μm) and nylon 6 (average diameter of 30 μm) by RIG followed by treatment of both grafted precursors with NMDG yielding fibrous adsorbents with almost 10 times smaller diameters than commercial granular resins (average particle diameters >300 μm). This led to more than twofolds faster kinetics coupled with about 20% improvement in boron adsorption capacity. Despite such performance improvement, there is still a room for enhancing the performance and overcoming mass transfer limitation of boron in microfibrous adsorbents by grafting onto nanofibrous substrates.

Electrospinning is a promising fiber-forming technique for obtaining polymeric fibers with controlled diameters ranging from few hundreds of nanometers to a few micrometers [24]. Thus, various polymers can be electrospun through this facile and low-cost technique with potential for applications in chemical treatment of wastewater [25]. Among all polymers, poly(vinylidene fluoride) (PVDF) is a thermoplastic that is known for its high elasticity and good processability, polymorphism, chemical stability, formation of stable radicals when exposed to high energy radiation and electrospinnability lending this material numerous applications [26]. Thus, PVDF and its nanofibers were developed as high-performance membranes for application in distillation, membrane contactor, and wastewater treatment [27,28]. However, the use of PVDF nanofibers for development of adsorbents for boron removal from solution is very scarce. Moreover, applying RIG as technique with its advantages for preparation of such adsorbent is rather rare. In a preliminary study, PVDF was electrospun under controlled conditions [29] followed by RIG of GMA and subsequent treatment with NMDG [30].

The objective of this study is to investigate the boron removal characteristics of the new adsorbent having nanofibrous structure obtained by RIG of GMA onto electrospun PVDF nanofibers followed by functionalization with NMDG. Particularly, the adsorption experimental data obtained under various conditions such as pH, initial solution concentration, and contact time were investigated systematically to establish the equilibrium isotherms, kinetics, and thermodynamics for boron adsorption on the new adsorbent. The mechanism of the boron adsorption by the prepared fibrous adsorbent was further investigated.

2. Methodology

2.1. Materials

PVDF powder supplied by Aldrich (M_w = 534,000, d = 1.74 g/cm^3, mp = 165°C) was used for preparation of electrospinning solutions. *N*,*N*-dimethylformamide (DMF, 99.5%) and acetone (99.7%) were purchased form Merck (Germany). GMA (monomer purity ≥ 99%) and tetrahydrofuran (anhydrous ≥ 99.9%) were supplied by Sigma-Aldrich (U.S.A.). Ethanol, propanol, methanol, and butanol (EMSURE® ACS) were obtained from Merck Millipore (Germany). NMDG (purity ≥ 99%) was purchased from Sigma-Aldrich. All the chemicals were used as received without any further purification. Deionized water (DI) obtained from a water purifier (NANO pure1 Diamond™) was used to prepare all boron solutions.

The synthetic wastewater containing boron with concentration of 1,000 mg/L was prepared by dissolving 5.716 g of H_3BO_3 in the distilled water and diluted to 1,000 mL and used as a stock solution. Standard solutions of boron (0.1, 1.0, 3.0, 5.0, 8.0 and 10.0 mg/L) were used to prepare a calibration curve, which was linear with a correlation coefficient above 0.999. The pH of the solution was adjusted using HCl (1M) and NaOH (1M) solutions.

2.2. Preparation of nanofibrous adsorbent

The PVDF solution of 15 wt% concentration was prepared by dissolving the polymer powder in a mixture of DMF and acetone at 8:2 (v/v) ratio under continuous stirring for an hour at 70°C. The PVDF solution was electrospun under optimized electrospinning parameters of 0.3 mL/h flow rate, 14.5 kV voltage, 25°C temperature, and 15 cm tip-to-collector distance following the procedure reported elsewhere [29].

The PVDF nanofibrous samples were immersed in a beaker containing 10% GMA in methanol for 12 h prior to irradiation. The GMA-saturated samples were transferred into PE zipper locked bag and deaerated with N_2 gas to remove oxygen. The samples were irradiated to a total dose of 100 kGy using an EB accelerator (EPS 3000) with an accelerating voltage of 1.0 MeV and beam current of 10 mA. Subsequently, the grafted samples were washed repeatedly using methanol to remove the remaining monomer and any formed homopolymer. The grafted fibers were dried using a vacuum oven for 20 h at 50°C, and their weight increase was calculated. The degree of grafting (DG) was determined using the following equation:

$$\text{DG (\%)} = [(W_g - W_o)/W_o] \times 100 \quad (1)$$

where W_o and W_g are the weights before and after grafting, respectively.

Poly(GMA)-grafted PVDF nanofibrous samples were treated with NMDG under continuous stirring and reflux. The optimum reaction parameters for poly(GMA)-grafted PVDF with 150% DG were 15% NMDG concentration, 87.0°C reaction temperature, and 65 min reaction time. After the reaction completion, the functionalized nanofibers were washed with DI few times and dried under vacuum for 20 h at 40°C. Details on the optimization of the reaction parameters were reported in a previous study [30]. The density of the glucamine group in the nanofibrous adsorbent was calculated according to the following formula:

$$\text{Density of glucamine}\left(\frac{\text{mmol}}{\text{g, adsorbent}}\right)=\frac{\left(\frac{Z_f-Z_i}{Z_f}\right)}{M}\times 1000 \quad (2)$$

where Z_i and Z_f are the weights of the initial grafted fibers and final functionalized fibers, whereas M is the molecular weight of the NMDG.

2.3. Adsorption equilibrium studies under different pH and boron concentrations

The effect of pH of the solution on the boron adsorption was performed by taking 0.8 g samples of the adsorbent and adding them to 150 mL of 100 mg/L of boric acid solution in Erlenmeyer flasks. The desired value of pH was adjusted by using 1 M HCl and 1 M NaOH solutions and varied in range of 3–11. A magnetic stirrer which was set to a temperature of 30°C and a speed of 200 rpm was used to stir the solution. All the reported adsorption data are an average of 3 data point.

The determination of adsorption isotherms under various concentrations was conducted by adding a fixed weight of the adsorbent (0.8 g) to Erlenmeyer flasks containing 150 mL boric acid solution with concentrations in the range of 50–250 mg/L. The mixture in the flask was stirred using a magnetic stirrer at 200 rpm for 3 h. The temperature and pH of the solution were fixed at 30°C and 7, respectively. The following equation was used to calculate the adsorption capacity at equilibrium, q_e (mg/g) [31]:

$$q_e(\text{mg/g})=\frac{(C_o-C_e)\times V}{m} \quad (3)$$

where C_o and C_e represent boron concentrations in the liquid phase at initial and equilibrium stages, respectively. V represents the volume of the solution (L) and m represents the adsorbent mass (g).

For the kinetic studies, a 0.8 g of the adsorbent was added to Erlenmeyer flasks. The flasks were filled earlier with 150 mL boric acid solution with concentrations ranging from 50 to 200 mg/L. The stirring speed was set at 200 rpm, whereas the pH and the temperature of the solution were maintained at 7 and 30°C, respectively. The equilibration time was varied in the range of 10–180 min. Finally, the samples were removed and the solution was analyzed for the residual boron concentration. In all the adsorption experiments, freshly prepared adsorbent samples were used. The boron concentration in solutions was determined using inductively coupled plasma, inductively coupled plasma – optical emission spectrometry by means of a PerkinElmer, Optima 7300 DV, USA, at a plasma gas flow of 15 L/min, auxiliary gas flow of 0.5 L/min, nebulizer gas flow of 0.7 L/min, and pump rate of 0.5 L/min.

3. Results and discussion

3.1. Nanofibrous adsorbent properties

The new fibrous boron chelating adsorbent that was prepared by RIG copolymerization of VBC onto nanofibrous PVDF substrate yielded poly(GMA)-grafted fibers with a DG of 150% , which was functionalized with NMDG imparting a glucamine density of 2.2 mmol/g to the adsorbent. The properties of the prepared fibrous adsorbent are summarized in Table 1. The mechanism by which the glucamine group captures boron from solution through coordination is shown in Fig. 1.

The effect of solution pH on the adsorption of boron was investigated to determine the optimum pH value to facilitate the determination of the adsorption mechanism. Fig. 2 illustrates the variation of the amount of boron adsorbed at equilibrium as a function pH. A gradual increase in the boron adsorption can be observed from pH 3 to 5, beyond which the increase tend be insignificant up to 7 at which the highest

Table 1
Properties of the prepared fibrous boron chelating adsorbent

Properties	Nanofibrous chelating adsorbent
Substrate	PVDF nanofibers
Moeity	NMDG
Chemical structure	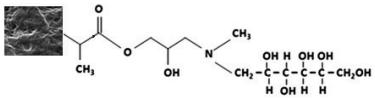
Density of NMDG	2.20 mmol/g-adsorbent
Water content	30%–40%
Average fiber diameter	*ca*. 500 ± 100 nm

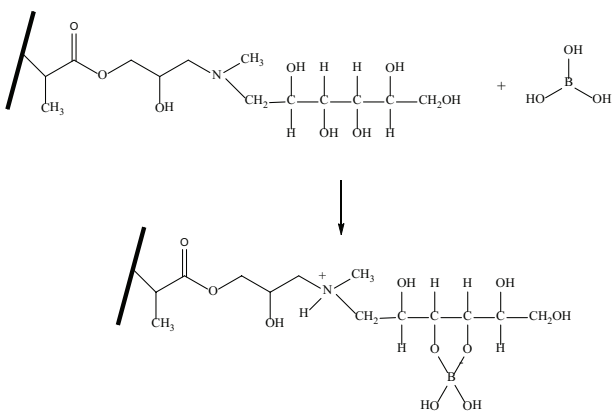

Fig. 1. The complexation of boron on NMDG-functionalized PVDF nanofibrous adsorbent.

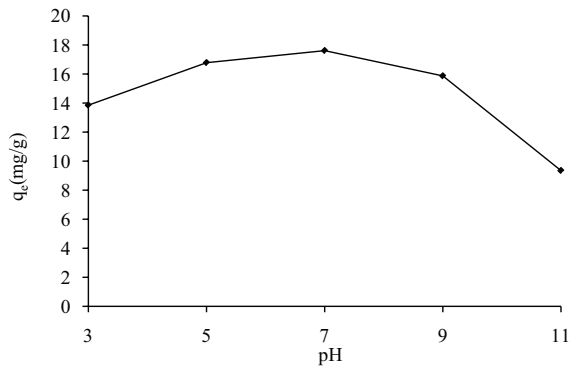

Fig. 2. Effect of pH on boron removal using newly synthesised nanofibrous adsorbent (concentration: 100 mg/L, adsorbent dosage: 0.8 g, time: 2 h, volume: 150 mL, stirring speed: 200 rpm and temperature: 30°C) (SD is in the range of 1.4%–2.3%).

adsorption value was obtained. Further increase in pH led to a marginal decrease at pH 9 followed by a remarkable decrease at 11. Similar trend was reported for the adsorption of boron from solutions onto microfibrous adsorbent containing NMDG based on radiation-grafted poly(GMA)/polyethylene (non-woven fabric) [32]. This behavior can be understood based on the fact that the distribution of $B(OH)_3$ and $B(OH)^{-4}$ species is controlled by pH of the solution, both of which compete for the adsorption on NMDG group available. Therefore, lower boric acid complexation is observed at low pH values wherein the $B(OH)_3$ species predominate [33,34]. More boron gets complexed to the adsorbent with the change of pH from 3 to 7. The decrease in the adsorption capacity of boron observed after pH 7 and above is most likely caused by the increase in the amount of the competing hydroxyl ions in the solution leading to a reduction in the adsorbent affinity toward boron. The results suggest that high selectivity for boron adsorption on the new adsorbent can be achieved at pH in the range of 5–9 with the maximum value can be attained at pH 7. The corresponding pH trend for commercial resins such as Diaion CRB 02 and Amberlite IRA 743 was in the range 6–10 [14,35]. It can be suggested that boron could be removed by the present glucamine-containing fibrous adsorbent almost in all pH range, but higher removal efficiency can be achieved at pH in the range of 6–8 with the maximum value obtained at pH 7. Therefore, pH 7 was chosen for all subsequent adsorption experiments. These findings are in a complete agreement with previous studies applied glucamine-functionalized adsorbents of various types such as macro porous particle [36], resins [37], and fibers [22].

3.2. Adsorption isotherm

The boron adsorption characteristics of the newly prepared nanofibrous adsorbent were evaluated by studying the adsorption isotherms using the three most well-established equilibrium models, that is, Langmuir, Freundlich, and Redlich–Peterson. The following equation represents the Langmuir isotherm model [38]:

$$\frac{C_e}{q_e} = \frac{1}{Q_L}(C_e) + \frac{1}{K_L Q_L} \tag{4}$$

where C_e (mg/L) represents the concentration in the liquid phase at equilibrium, q_e is the boron adsorption at equilibrium, while Q_L (mg/g) and K_L (L/g) are the Langmuir adsorption constants related to the adsorption capacity and adsorption energy, respectively.

The Freundlich isotherm model is described by the following equation [39]:

$$\log(q_e) = \frac{1}{n}\log C_e + \log K_F \tag{5}$$

where q_e represents the boron adsorption at equilibrium, C_e (mg/L) is the concentration in the liquid phase at equilibrium, while K_F (mg/g)(L/mg)$^{1/n}$ and $1/n$ are the Freundlich adsorption constant and heterogeneity factor indicating the adsorption intensity, respectively [40].

The Redlich–Peterson isotherm has incorporated features of both Langmuir and Freundlich isotherms [41] and represented by the following model [39]:

$$\ln(K_R \frac{C_e}{q_e} - 1) = g\ln(C_e) + \ln(A_R) \tag{6}$$

where C_e (mg/L) is the concentration in the liquid phase at equilibrium, q_e represents the boron adsorption at equilibrium, while K_R (L/g) and A_R (1/mg) are Redlich–Peterson isotherm constants, and g is the isotherm exponent which has values between 0 and 1.

The equilibrium isotherms for boron adsorption by the new nanofibrous adsorbents are presented in Figs. 3–5 whereas the best-fit data obtained from the model parameters estimated from Eqs. (4)–(6) are presented in Table 2. It can be observed that the newly prepared nanofibrous adsorbent is best fitted to Redlich–Peterson isotherm (r^2 = 0.993) compared with the other two models: Langmuir isotherm (r^2 = 0.959) and Freundlich isotherm (r^2 = 0.828). The coefficients obtained from Redlich–Peterson model were used to verify the fitting provided by the Langmuir and Freundlich isotherms. The high g value of >0.9 supports the suitability of Langmuir isotherm to fit the experimental data [39]. This suggests the presence of a monolayer adsorption on the homogeneous sites [42]. This is clearly consistent with the chemical adsorption nature of boron complexation by the NMDG ligands on Amberlite IRA 743 resin and microfibrous adsorbent reported earlier [3,22].

3.3. Adsorption kinetics

The adsorption kinetics of boron on the nanoadsorbent was tested with pseudo-first-order and pseudo-second-order models. The fitting of the experimental data with model-predicted value is determined by the correlation coefficient (r^2), and the applicability of the kinetic model to describe the adsorption process was confirmed using the normalized standard deviation given in Eq. (7):

$$\Delta q = 100 \times \sqrt{\frac{\Sigma[(q_{\exp} - q_{\text{cal}}) / q_{\exp}]^2}{n-1}} \tag{7}$$

where n is the number of data points and q_{exp} (mg/g) and q_{cal} (mg/g) are the experimental and calculated adsorption capacities, respectively.

According to the pseudo-first-order model, the rate of adsorption is proportional to the number of the unoccupied adsorption sites as represented in the following expression [43]:

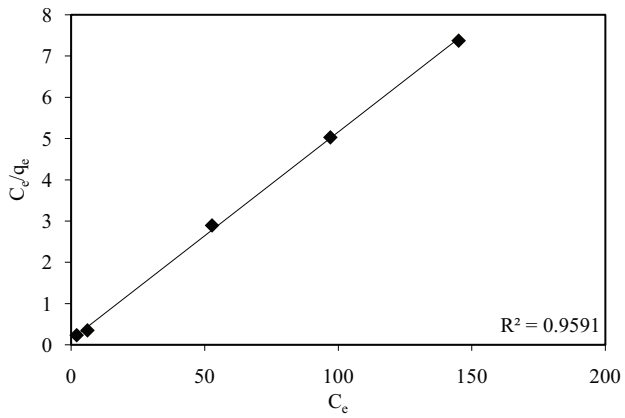

Fig. 3. Langmuir isotherm plot of boron adsorption on boron chelating nanofibrous adsorbent.

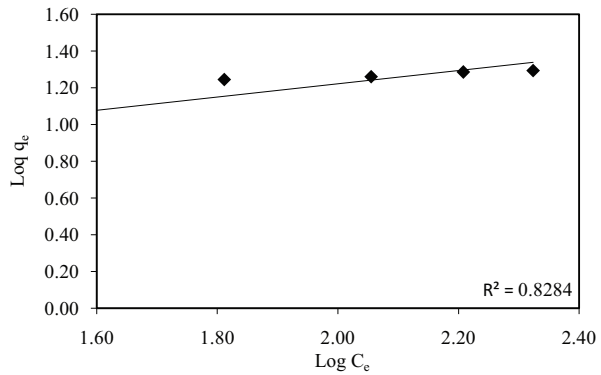

Fig. 4. Freundlich isotherm plot of boron adsorption on boron chelating nanofibrous adsorbent.

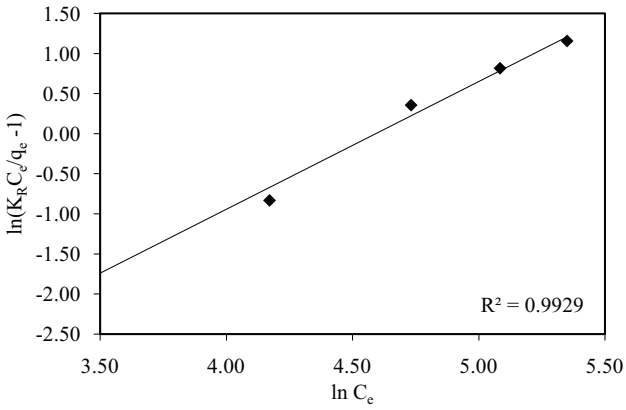

Fig. 5. Redlich–Petterson isotherm plot of boron adsorption on boron chelating nanofibrous adsorbent.

$$q_t = q_e\left(1-\exp^{-k_1 t}\right) \tag{8}$$

where q_e is the amount of boron adsorbed at equilibrium (mg/g), q_t is the amount of boron adsorbed at t time (mg/g), and k_1 is the rate constant of the pseudo-first-order sorption (min^{-1}).

Fig. 6 shows plots of for the pseudo-first-order model for the adsorption of boron, and its parameters are presented in Table 3. The estimated equilibrium sorption values for solutions with concentrations ranging from 50 to 200 mg/L were found to deviate from the corresponding experimental values by 6.5%–8.7%. This was coupled with a low linearity as indicated by r^2 values that were found to be in the range of 0.891–0.928. The drop in r^2 value from 0.904 (for 50 mg/L concentration) to 0.891 (for 75 mg/L concentration) for the pseudo-first-order model is likely due to an experimental error. This suggests that pseudo-first-order model is inadequate describing the adsorption kinetics of boron on the new nanofibrous adsorbent.

Table 2
Isotherm models' parameters for sorption of boron on newly prepared fibrous adsorbent

Isotherm		Fibrous chelating adsorbent
Langmuir	Q_L (mg/g)	19.881
	K_L (L/mg)	0.041
	r^2	0.959
Freundlich	K_F (mg/g) (L/mg)$^{1/n}$	2.769
	n	3.159
	r^2	0.828
Redlich–Peterson	A_R (mg^{-1})	0.00067
	K_R (L/g)	0.39
	g	1
	r^2	0.9929

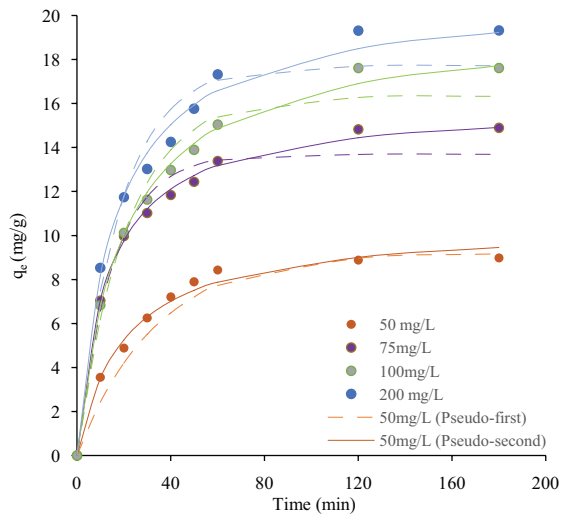

Fig. 6. Kinetic models for boron adsorption on new nanofibrous adsorbent.

Table 3
Kinetic parameters for adsorption of boron on nanofibrous adsorbent

Type	Parameters	50 mg/L	75 mg/L	100 mg/L	200 mg/L
Pseudo-first-order	r^2	0.904	0.891	0.928	0.917
	$q_{e,\text{calc}}$ (mg/g)	9.208	13.695	16.329	17.721
	k_1 (g/mg min)	0.030	0.070	0.048	0.055
	Δq (%)	8.275	6.522	7.057	8.690
Pseudo-second-order	r^2	0.967	0.996	0.990	0.976
	$q_{e,\text{calc}}$ (mg/g)	10.512	16.164	19.609	20.894
	k_2 (g/mg min)	0.005	0.005	0.003	0.003
	h (mg/g min)	0.524	1.250	1.022	1.341
	Δq (%)	4.827	1.949	2.356	4.111
Experiment	$q_{e,\text{exp}}$ (mg/g)	12.04	14.89	17.61	19.32

Pseudo-second-order model [44] described that the rate of sorption is proportional to the square of the number of the unoccupied adsorptive sites and can be expressed as follows:

$$q_t = \frac{k_2 q_e^2 t}{1 + k_2 q_e t} \tag{9}$$

where q_e is the amount of solute adsorbed at equilibrium (mg/g), q_t is the amount of solute adsorbed at t time (mg/g), and k_2 is the pseudo-second-order rate constant of sorption (g/mg min).

The initial adsorption rate, h (mg/g min), of the pseudo-second-order model at $t \to 0$ is given as follows:

$$h = kq_e^2 \tag{10}$$

The h (mg/g min) value can be determined experimentally from the slope and intercept of the plots.

Fig. 6 presents plots of the pseudo-second-order model for the adsorption of boron, and the rate parameters are presented in Table 3. The obtained r^2 values were higher than 0.96 whereas, the calculated q_e values were close to the experimental ones as indicated by the lower normalized standard deviation, and Δq values were in the range of 1.9%–4.8%. This suggests that the adsorption kinetics of boron onto the fibrous adsorbent can be well described by the pseudo-second-order model. The consistency of the adsorption experimental data with the pseudo-second-order kinetic model signifies that the adsorption is dominated by chemical adsorption involving monolayer adsorption in which valence forces through sharing or exchange of electrons between sorbent and sorbate [45]. This trend is similar to previous studies, which used various glucamine-functionalized adsorbents such as resins and cellulose-based fibers [31], porous particles [46], PE-PP microfibers [47], and radiation-grafted nylon microfibers [22].

The initial adsorption rate, h, was found to have a positive linear relationship against the initial boron concentrations varying from 50 to 200 mL/L. This suggests that at the low initial concentration, the numbers of boron molecules to be adsorbed are limited to the available active sites on the adsorbent. As the initial concentrations increased, the numbers of boron molecules in the solution are also increased leading to the adsorption of more boron molecules on the active sites.

3.4. Adsorption mechanism

The Weber–Morris intraparticle diffusion model was used to obtain a better understanding of the boron removal mechanism of the prepared adsorbent. The model is expressed by the following equation [48]:

$$q_t = k_{\text{pi}} t^{0.5} + C_i \tag{11}$$

where k_{pi} (mg/g·min$^{0.5}$) is the intraparticle diffusion rate constant of stage i, and C_i (mg/g) is the intercept of stage i obtained from the plot of q_t vs. $t^{0.5}$. The C_i values provide information about the thickness of the boundary layer, that is, the larger the intercept, the greater the boundary layer effect. It has been reported that it is essential for the q_t vs. $t^{0.5}$ plot to cross the origin if the sole rate-controlling step is the intraparticle diffusion. If the plot is found to intercept at a value that is not zero, it can be established that both intraparticle and boundary layer diffusion are controlling the adsorption, which has a chemisorption nature.

Because the plot does not intercept at zero, the plot tends to present a multi-linear behavior as is depicted in Fig. 7. These results suggest that two or more steps occur in the adsorption processes, involving instantaneous adsorption on the external surface, intraparticle diffusion or gradual adsorption being the rate-controlling stage, and the final equilibrium stage where the intraparticle diffusion slows down due to the decrease of adsorption sites and the low concentration of adsorbate left in the aqueous solution [49] This multi-linear behavior exhibited is going along with the study conducted on the removal of anionic dye (eosin Y) using ethylenediamine-modified chitosan, in which it was established that after the first stage (external surface adsorption) is completed fast and less apparent, only the second stage (intraparticle diffusion) and the third stage (equilibrium)

are prevailed [50]. The steps observed in this study are also similar to the adsorption mechanism reported for boron adsorption on microfibers grafted with poly(VBC)/NMDG ligands. This fibrous adsorbent also reached the equilibrium stage at a faster rate than the granular resin [22].

At all initial concentrations, k_{p1} was higher than $k_{p2,}$ and C_2 was larger than C_1 as depicted from data shown in Table 4. This indicates that the rate of boron removal is higher in the beginning due to the large surface area of the adsorbent available for the adsorption of borate ions. After the adsorbed material formed a thick layer (caused by the interionic attraction and molecular association), the capacity of the adsorbent became exhausted and the uptake rate was controlled by the rate at which the adsorbate was transported from the exterior to the interior sites of the adsorbent particle [51].

The plots of q_t vs. $t^{0.5}$ show two stages of linearity of boron sorption onto the adsorbent are associated with intraparticle diffusion and equilibrium stages. The external surface adsorption was less apparent, and this could be attributed to rapid diffusion of boron onto the external surface of adsorbent. This indicates that the first stage of diffusion is very rapid and almost instantaneous for nanofibrous adsorbents when compared with microfibrous and granular adsorbents. This can be attributed to the decrease in the size and subsequent increase in the surface area of the adsorbent. Plots of q_t vs. $t^{0.5}$ for adsorption of boron on microfibrous adsorbent showed three stages of linearity representing the diffusion of onto the external surface, intraparticle diffusion, and equilibrium diffusion [22]. It can be suggested that the newly synthesized adsorbent provides higher specific surface area, and thus lesser time for the diffusion of target ions was reduced. This coincided with rise in the number of functional groups caused by higher NMDG density leading to larger number of sorption sites faster the adsorption rate.

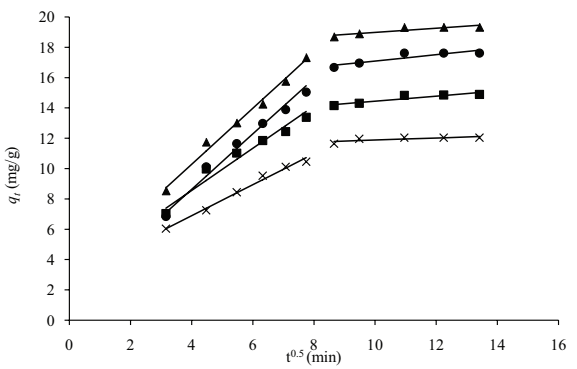

Fig. 7. Intraparticle diffusion model for boron adsorption on the nanofibrous adsorbent.

3.5. Adsorption thermodynamics

Thermodynamic investigation was performed to determine the driving force of entropy change in a system that is kept isolated and to conclude if the adsorption process is spontaneous or not. The fundamental criterion of spontaneity is the Gibbs free energy change, $\Delta G°$. If $\Delta G°$ is negative in value, spontaneous reaction occurs at a given temperature. The Gibbs free energy change ($\Delta G°$), enthalpy change ($\Delta H°$), and entropy change ($\Delta S°$), which are all thermodynamic parameters, can be ascertained from the changes in the thermodynamic equilibrium constant (K_D) and temperature (T). These can be acquired using Eq. (12) [45]:

$$\Delta G° = -RT\ln K_D \tag{12}$$

where R represents a gas constant, which equals 8.314 J/mol K, K_D represents the equilibrium constant, while T (K) represents the medium temperature. The K_D value is acquired using Eq. (13) as follows [45]:

$$K_D = \frac{C_o - C_e}{C_e} \cdot \frac{V}{m} \tag{13}$$

where C_o represents the initial concentration (mg/L), C_e represents the equilibration concentration after adsorption (mg/L), while V and m represent the volume of the solution (L) and the dose of the membrane (g), respectively. $\Delta H°$ and $\Delta S°$ of adsorption are acquired using Eq. (14) [45]:

$$\ln K_D = -\frac{\Delta G°}{RT} = -\frac{\Delta H°}{RT} + \frac{\Delta S°}{R} \tag{14}$$

$\Delta H°$ and $\Delta S°$ were calculated from the slope and intercept of a plot of $\ln K_D$ against $1/T$.

The free energy changes ($\Delta G°$) at 293, 303 and 313 K temperatures were –0.228, –0.153, and –0.81 kJ/mol, respectively. Such negative values suggest that the adsorption of the borate ions onto nanofibrous adsorbent was thermodynamically feasible and spontaneous. This reveals an increased randomness at the solid–solution interface during the immobilization of boron on the active sites of the nanofibrous adsorbent. The decrease in the negative values of $\Delta G°$ with the increase in the temperature suggests the adsorption process of boron on the newly prepared nanofibrous adsorbent is spontaneous.

The obtained $\Delta H°$ was 2.4 kJ/mol, and such positive value further indicates that the adsorption of boron was

Table 4
Intraparticle diffusion parameters for the adsorption of boron on nanofibrous adsorbent

Initial concentration C_0 (mg/L)	k_{p1} (mg/g min$^{0.5}$)	C_1	R_{p1}^2	k_{p2} (mg/g min$^{0.5}$)	C_2	R_{p2}^2
50	1.107	0.59	0.99	0.068	8.145	0.34
75	1.389	3.00	0.96	0.167	12.77	0.83
100	1.825	1.33	0.98	0.207	15.02	0.75
200	1.847	2.89	0.99	0.138	17.59	0.76

Table 5
Comparison between nanofibrous, microfibrous adsorbents and granular resins

Properties	Granular resin, Diaion CRB 03 [22]	Microfibrous adsorbent [22]	Nanofibrous adsorbent in this study
Physical form	Granular	Microfibrous adsorbent	Nanofibrous adsorbent
Chelating group	NMDG	NMDG	NMDG
Particle/fiber diameter	350–550 μm	30 μm	0.5 μm
Highest adsorption capacity	11.6 mg-B/g-ads[a]	13.8 mg-B/g-ads[a]	17.6 mg-B/g-ads[a]

[a]Conditions: batch mode, 100 mg/L initial concentration and pH 7 in all experiments.

endothermic in nature, and the adsorption capacity increases with the temperature increase. The determined $\Delta S°$ value was 3.1 J/mol·K, and this positive value indicates the presence of spontaneity at the solid–solution interface during the adsorption of boron in aqueous solution on the nanofibrous adsorbent. A similar behavior was also observed for NMDG-functionalized silica-polyallylamine composites [35] and microfibers [22]. It can therefore be concluded that the adsorption of boron on the newly prepared nanofibrous adsorbent follows a chemical adsorption process which is online with the investigated adsorption isotherms and kinetics.

3.6. Comparison between fibrous chelating adsorbents and granular resins

A comparison between the newly prepared nanofibrous adsorbent, microfibrous adsorbent, and a commercial granular resin is presented in Table 5. For instance, the difference in shape and size of the three adsorbents seems to have remarkable impact the boron adsorption capacity under the same conditions. Fibrous adsorbents have higher surface area resulting in higher adsorption capacities than the granular adsorbent, and such effect is more profound with nanofibrous adsorbent. The nanofibrous adsorbent also demonstrated a higher intraparticle diffusion rate constant of 1.825 mg/g $min^{0.5}$ (at initial boron concentration 100 mg/L) compared with 1.134 mg/g $min^{0.5}$ for the microfibrous adsorbent and 0.662 mg/g $min^{0.5}$ for the granular Diaon CRB 03 [22], respectively. Hence, it can be concluded that the adsorption operation time can be reduced, and bigger volume of water contaminated with boron can be treated with the use of the nanofibrous adsorbent prepared in this study.

The nanofibrous adsorbent showed good stability and reusability as reported in a previous study involving treatments with 1 M HCl and 1 M NaOH solutions [30]. The adsorbent retained same boron adsorption capacity after five cycles of adsorption–desorption cycles (data are not shown here). It can therefore be suggested that the newly prepared boron chelating nanofibrous adsorbent has a strong potential for application in boron removal from aqueous solutions.

4. Conclusion

A new nanofibrous chelating adsorbent with glucamine density of 2.2 mmol was successfully prepared by RIG of GMA onto electrospun PVDF nanofibers followed by functionalization with NMDG. The obtained nanofibrous adsorbent was tested for boron removal from solutions and delivered the highest adsorption value at pH 7. The adsorption equilibrium data for boron adsorption were well-described by Redlich–Peterson isotherm model, whereas the kinetic behavior was well-fitted to the pseudo-second-order model suggesting the presence of chemisorption. The boron adsorption mechanism was represented by Weber–Morris model. Hence, it can be suggested that the adsorption mechanism involves instantaneous adsorption on the external surface and intraparticle diffusion or gradual adsorption (the rate-controlling step) prior to reaching the final equilibrium stage. The intraparticle diffusion rate constant of the prepared adsorbent was found to be higher (1.825 mg/g·$min^{0.5}$) than not only that of microfibrous adsorbent (1.134 mg/g $min^{0.5}$) but also the commercial resin (0.662 mg/g·$min^{0.5}$). The adsorption thermodynamic investigation suggested that a spontaneous adsorption took place on the surfaces of the nanofibrous adsorbent. It can be finally concluded that the nanofibrous adsorbent obtained in this study has higher adsorption capacity and faster kinetics than both commercial granular commercial resins and microfibrous adsorbents.

Acknowledgment

The authors acknowledge the financial support by Y-UTP cost center 015LCO-065, Ministry of Higher Education (Malaysia) for FRGS (grant no. 4F878).

References

[1] M.M. Nasef, M. Nallappan, Z. Ujang, Polymer-based chelating adsorbents for the selective removal of boron from water and wastewater: a review, React. Funct. Polym., 85 (2014) 54–68.
[2] WHO, Guidelines for Drinking Water Quality, 4th ed., World Health Organization, Malta, Gutenberg, 2011.
[3] N. Ozturk, D. Kavak, Adsorption of boron from aqueous solutions using fly ash: batch and column studies, J. Hazard. Mater., 127 (2005) 81–88.
[4] S. Karahan, M. Yurdakoç, Y. Seki, K. Yurdakoç, Removal of boron from aqueous solution by clays and modified clays, J. Colloid Interface Sci., 293 (2006) 36–42.
[5] M.F. Chong, K.P. Lee, H.J. Chieng, I.I.S. Ramli, Removal of boron from ceramic industry wastewater by adsorption–flocculation mechanism using palm oil mill boiler (POMB) bottom ash and polymer, Water Res., 43 (2009) 3326–3334.
[6] A.E. Yilmaz, R. Boncukcuoglu, M.M. Kocakerim, M.T. Yilmaz, C. Paluluoglu, Boron removal from geothermal waters by electrocoagulation, J. Hazard. Mater., 153 (2008) 146–151.
[7] Y. Oren, C. Linder, N. Daltrophe, Y. Mirsky, J. Skorka, O. Kedem, Boron removal from desalinated seawater and brackish water by improved electrodialysis, Desalination, 199 (2006) 52–54.
[8] M. Turek, P. Dydo, B. Bandura-Zalska, Boron removal from dual-staged seawater nanofiltration permeate by electrodialysis, Desal. Wat. Treat., 10 (2009) 60–63.

[9] K.L. Tu, L.D. Nghiem, A.R. Chivas, Boron removal by reverse osmosis membranes in seawater desalination applications, Sep. Purif. Technol., 75 (2010) 87–101.
[10] N. Hilal, G.J. Kim, C. Somerfield, Boron removal from saline water: a comprehensive review, Desalination, 273 (2011) 23–35.
[11] J. Wolska, M. Bryjak, Methods for boron removal from aqueous solutions – a review, Desalination, 310 (2013) 18–24.
[12] M.-O. Simonnot, C. Castel, M. Nicolai, C. Rosin, M. Sardin, H. Jauffret, Boron removal from drinking water with a boron selective resin: is the treatment really selective?, Water Res., 34 (2000) 109–116.
[13] B.M. Smith, P. Todd, C.N. Bowman, Hyperbranched chelating polymers for the polymer-assisted ultrafiltration of boric acid, Sep. Sci. Technol., 34 (1999) 1925–1945.
[14] N. Badruk, M. Kabay, H. Demircioglu, U. Mordogan, U. Ipekoglu, Removal of boron from wastewater of geothermal power plant by selective ion exchange resins. II. Column sorption-elution studies., Sep. Sci. Technol., 34 (1999) 2981–2995.
[15] J.D. Lou, G.L. Foutch, J.W. Na, The sortion capacity of boron on anionic exchange resin, Sep. Sci. Technol., 34 (1999) 2923–2941.
[16] R.M. Roberts, Deboronation process by ion exchange, Ind. Eng. Chem. Prod. Res. Dev., 10 (1971) 356–357.
[17] H. Polat, A. Vengosh, I. Pankratov, M. Polat, A new methodology for removal of boron from water by coal and fly ash, Desalination, 164 (2004) 173–188.
[18] T.M. Ting, H. Hoshina, N. Seko, M. Tamada, Removal of boron by boron-selective adsorbent prepared using radiation induced grafting technique, Desal. Wat. Treat., 51 (2013) 2602–2608.
[19] K. Ikeda, D. Umeno, K. Saito, F. Koide, E. Miyata, T. Sugo, Removal of boron using nylon-based chelating fibers, Ind. Eng. Chem. Res., 50 (2011) 5727–5732.
[20] M.M. Nasef, O. Güven, Radiation-grafted copolymers for separation and purification purposes: status, challenges and future directions, Prog. Polym. Sci., 37 (2012) 1597–1656.
[21] M.M. Nasef, T.M. Ting, A. Abbasi, A. Layeghi-moghaddam, S.S. Alinezhad, K. Hashim, Radiation grafted adsorbents for newly emerging environmental applications, Radiat. Phys. Chem., 118 (2016) 55–60.
[22] T.M. Ting, M.M. Nasef, K. Hashim, Evaluation of boron adsorption on new radiation grafted fibrous adsorbent containing N-methyl-D-glucamine, J. Chem. Technol. Biotechnol., 91 (2016) 2009–2017.
[23] H. Parschová, E. Mištová, Z. Matějka, L. Jelínek, N. Kabay, P. Kauppinen, Comparison of several polymeric sorbents for selective boron removal from reverse osmosis permeate, React. Funct. Polym., 67 (2007) 1622–1627.
[24] D. Chen, Y.E. Miao, T.X. Liu, Electrically conductive polyaniline/polyimide nanofiber membranes prepared via a combination of electrospinning and subsequent in situ polymerization growth, ACS Appl. Mater. Interfaces, 5 (2013) 1206–1212.
[25] Y. Huang, Y.-E. Miao, T. Liu, Electrospun fibrous membranes for efficient heavy metal removal, J. Appl. Polym. Sci., 131 (2014) 40864.
[26] S.K. Kim, J.H. Ryu, H.D. Kwen, C.H. Chang, S.H. Cho, Convenient preparation of ion-exchange PVDF membranes by a radiation-induced graft polymerization for a battery separator, Polymer (Korea), 34 (2010) 126–132.
[27] F. Liu, N.A. Hashim, Y. Liu, M.R.M. Abed, K. Li, Progress in the production and modification of PVDF membranes, J. Membr. Sci., 375 (2011) 1–27.
[28] G.D. Kang, Y.M. Cao, Application and modification of poly(vinylidene fluoride) (PVDF) membranes – a review, J. Membr. Sci., 463 (2014) 145–165.
[29] M.L. Nallappan, M.M. Nasef, Optimization of elecrospinning of PVDF scaffolds fabrication using response surface method, J. Teknologi, 75 (2015) 103–107.
[30] M.L. Nallappan, M.M. Nasef, T.M. Ting, A. Ahmad, An optimized covalent immobilization of glucamine on electrospun nanofibrous poly(vinylidene fluoride) sheets grafted with oxirane groups for higher boron adsorption, Fibers Polym., 19 (2018) 1694–1705.
[31] S. Nishihama, Y. Sumiyoshi, T. Ookubo, K. Yoshizuka, Adsorption of boron using glucamine-based chelate adsorbents, Desalination, 310 (2013) 81–86.
[32] C. Irawan, Y.-L. Kuo, J.C. Liu, Treatment of boron-containing optoelectronic wastewater by precipitation process, Desalination, 280 (2011) 146–151.
[33] N. Geffen, R. Semiat, M.S. Eisen, Y. Balazs, I. Katz, C.G. Dosoretz, Boron removal from water by complexation to polyol compounds, J. Membr. Sci., 286 (2006) 45–51.
[34] K. Yoshimura, Y. Miyazaki, F. Ota, S. Matsuoka, H. Sakashita, Complexation of boric acid with the N-methyl-D-glucamine group in solution and in crosslinked polymer, J. Chem. Soc., Faraday Trans., 94 (1998) 683–689.
[35] X. Li, R. Liu, S. Wu, J. Liu, S. Cai, D. Chen, Efficient removal of boron acid by N-methyl-d-glucamine functionalized silica–polyallylamine composites and its adsorption mechanism, J. Colloid Interface Sci., 361 (2011) 232–237.
[36] L. Wang, T. Qi, Z. Gao, Y. Zhang, J. Chu, Synthesis of N-methylglucamine modified macroporous poly(GMA-co-TRIM) and its performance as a boron sorbent, React. Funct. Polym., 67 (2007) 202–209.
[37] H. Liu, X. Ye, Q. Li, T. Kim, B. Qing, M. Guo, F. Ge, Z. Wu, K. Lee, Boron adsorption using a new boron-selective hybrid gel and the commercial resin D564, Colloids Surf., A, 341 (2009) 118–126.
[38] G. Limousin, J.P. Gaudet, L. Charlet, S. Szenknect, V. Barthès, M. Krimissa, Sorption isotherms: a review on physical bases, modeling and measurement, Appl. Geochem., 22 (2007) 249–275.
[39] K.Y. Foo, B.H. Hameed, Insights into the modeling of adsorption isotherm systems, Chem. Eng. J., 156 (2010) 2–10.
[40] H.M.F. Freundlich, Over the adsorption in solution, J. Phys. Chem., 57 (1906) 385–471.
[41] O. Redlich, D.L. Peterson, A useful adsorption isotherm, J. Phys. Chem., 63 (1959) 1024–1026.
[42] R.I. Yousef, B. El-Eswed, A.a.H. Al-Muhtaseb, Adsorption characteristics of natural zeolites as solid adsorbents for phenol removal from aqueous solutions: kinetics, mechanism, and thermodynamics studies, Chem. Eng. J., 171 (2011) 1143–1149.
[43] S. Lagergren, Zur theorie der sogenannten adsorption geloster stoffe, Kungliga Svenska Vetenskapsakademiens, Handlingar Band, 24 (1898) 1–39.
[44] Y.S. Ho, Adsorption of Heavy Metals from Waste Streams by Peat, University of Birmingham, UK, Birmingham, 1995.
[45] H.K. Boparai, M. Joseph, D.M. O'Carroll, Kinetics and thermodynamics of cadmium ion removal by adsorption onto nano zerovalent iron particles, J. Hazard. Mater., 186 (2011) 458–465.
[46] S. Samatya, A. Tuncel, N. Kabay, Boron removal from geothermal water by a novel monodisperse porous poly(GMA-co-EDM) resin containing N-methyl-D-glucamine functional group, Solvent Extr. Ion Exch., 30 (2012) 341–349.
[47] T.M. Ting, M.M. Nasef, Modification of polyethylene-polypropylene fibers by emulsion and solvent radiation grafting systems for boron removal, Fibers Polym., 18 (2017) 1048–1055.
[48] W.J. Weber, J.C. Morris, Kinetics of adsorption on carbon from solution, J. Sanit. Eng. Div., Am. Soc. Civil Eng. Proc., 89 (1963) 31–59.
[49] A. Arslantas, D. Sinirlioglu, F. Eren, A.E. Muftuoglu, A. Bozkurt, An investigation of proton conductivity of PVDF based 5-aminotetrazole functional polymer electrolyte membranes (PEMs) prepared via direct surface-initiated AGET ATRP of glycidyl methacrylate (GMA), J. Polym. Res., 21 (2014) 437.
[50] S. Chatterjee, S. Chatterjee, B.P. Chatterjee, A.R. Das, A.K. Guha, Adsorption of a model anionic dye, eosin Y, from aqueous solution by chitosan hydrobeads, J. Colloid Interface Sci., 288 (2005) 30–35.
[51] M. Bhaumik, A. Maity, V.V. Srinivasu, M.S. Onyango, Removal of hexavalent chromium from aqueous solution using polypyrrole-polyaniline nanofibers, Chem. Eng. J., 181 (2012) 323–333.